

## Attractive Hubbard model on a triangular lattice

Raimundo R. dos Santos\*

*Departamento de Física, Pontifícia Universidade Católica do Rio de Janeiro, Caixa Postal 38071,  
22452-970 Rio de Janeiro, Brazil*

(Received 28 January 1993)

We study the attractive (i.e., negative- $U$ ) Hubbard model on a triangular lattice. A strong-coupling analysis indicates that a charge-density-wave (CDW) state cannot be formed for any band filling due to frustration, while pairing correlations are robust. Quantum Monte Carlo simulations confirm the absence of a CDW state for intermediate couplings, and show that the critical temperature for superconductivity is higher close to half-filling, unlike the square lattice. Also, the behavior of the uniform magnetic susceptibility suggests that the precursor spin-gap phase is not affected by frustration.

### I. INTRODUCTION

The formation of local (or real-space) electron pairs is believed to be relevant to explain a variety of phenomena such as unconventional properties in some superconducting materials, the existence of charge-density waves in narrow-band systems, the properties of negative- $U$  centers in semiconductors, polymer conductivity, and heavy-fermion superconductivity; see Ref. 1 for a list of references. Electron pairs may be formed in narrow-band systems due to a local attractive short-ranged effective interaction, which in turn can be explained through microscopic mechanisms such as electronic coupling to either local phonon modes<sup>2</sup> or to internal degrees of freedom (excitons, plasmons, or other electronic subsystems<sup>3-6</sup>). The Hubbard model with on-site attractive (i.e., negative- $U$ ) interaction contains the basic ingredients to describe these systems, though in some cases a nearest-neighbor interaction must also be included to account for the observed properties.<sup>1</sup>

Recently, this model has been the subject of renewed interest,<sup>7-11</sup> motivated by the short coherence lengths of superconducting electron pairs in high- $T_c$  ceramic materials and by a suggestion that superconductivity in buckminster fullerenes could be explained along similar lines.<sup>12</sup> As a result of mappings onto different models and several calculations, the following picture emerges for the attractive Hubbard model on bipartite lattices:<sup>1,7,8</sup> Superconductivity sets in at a critical temperature  $T_c$ , which depends on the band filling and on  $U$ . Two regimes of  $U$  should be distinguished: For weak coupling, with lower  $T_c$ , the system goes from a high-temperature normal metallic state to a superconductor; for strong coupling, the transition corresponds to a condensation of preformed pairs (in the spin-gap phase<sup>11</sup>) into a state with long-range order. At half-filling ( $\rho = 1$ ), a charge-density-wave (CDW) state coexists with the superconducting state.<sup>1,7,8</sup> On a square lattice and at half-filling, one then has  $T_c = 0$  for any  $U < 0$ ; away from half-filling and for fixed  $U$ , the superconducting critical temperature rises sharply from zero, displaying a maximum at some intermediate filling, and falling again to zero as

$\rho \rightarrow 0$  or 2 (see Ref. 8).

The situation for nonbipartite lattices is less clear. For instance, some features found for the square lattice should be different on a triangular lattice as a result of frustration. With this in mind, here we study the attractive Hubbard model on a triangular lattice, by means of strong-coupling analyses and quantum Monte Carlo (MC) simulations. We focus on the interplay between CDW states and superconductivity, on the phase diagram  $T_c$  versus  $\rho$ , and on whether a spin-gap phase persists above  $T_c$ . The layout of the paper is as follows. In Sec. II we discuss particle-hole transformations and the strong-coupling limits of both the attractive and repulsive models. In Sec. III we briefly outline the quantum Monte Carlo background as well as the finite-size scaling hypothesis for the pairing correlation functions. The results are displayed and discussed in Sec. IV, and Sec. V summarizes our findings.

### II. PARTICLE-HOLE TRANSFORMATIONS AND STRONG-COUPLING LIMITS

The Hubbard Hamiltonian can be written as

$$\mathcal{H} = -t \sum_{\langle i,j \rangle} (c_{i\sigma}^\dagger c_{j\sigma} + \text{H.c.}) + U \sum_i (n_{i\uparrow} - \frac{1}{2})(n_{i\downarrow} - \frac{1}{2}) - \mu \sum_{i,\sigma} n_{i\sigma}, \quad (1)$$

where the sums run over sites of a triangular lattice,  $\langle i, j \rangle$  denotes nearest-neighbor sites, H.c. stands for Hermitian conjugate, and  $c_{i\sigma}^\dagger$  ( $c_{i\sigma}$ ) creates (annihilates) a fermion at site  $i$  with spin  $\sigma$ ;  $U < 0$  is the attractive on-site interaction, and  $\mu$  is the chemical potential controlling the band filling. On a triangular lattice, the nearest-neighbor (NN) sites of a site located at the origin are located at  $\pm \mathbf{a}_1$ ,  $\pm \mathbf{a}_2$ , and  $\pm \mathbf{a}_3$ , with

$$\mathbf{a}_1 = \mathbf{x}, \quad \mathbf{a}_2 = \frac{1}{2} (\mathbf{x} + \sqrt{3}\mathbf{y}), \quad \mathbf{a}_3 = \frac{1}{2} (-\mathbf{x} + \sqrt{3}\mathbf{y}), \quad (2)$$

where  $\mathbf{x}$  and  $\mathbf{y}$  are the Cartesian unit vectors.

A *full* particle-hole transformation takes electrons with a given polarization into holes with the same polarization,

$$c_{j\sigma} \rightarrow \tilde{c}_{j\sigma}^\dagger = (-1)^j c_{j\sigma}, \quad (3)$$

such that

$$n_{j\sigma} \rightarrow \tilde{n}_{j\sigma} = 1 - n_{j\sigma}, \quad (4)$$

thus essentially preserving charge and spin degrees of freedom. The Hamiltonian (1) becomes

$$\begin{aligned} \tilde{\mathcal{H}} = & - \sum_{\substack{(i,j) \\ \sigma}} \tilde{t}_{ij} \left( \tilde{c}_{i\sigma}^\dagger \tilde{c}_{j\sigma} + \text{H.c.} \right) \\ & + U \sum_i \left( \tilde{n}_{i\uparrow} - \frac{1}{2} \right) \left( \tilde{n}_{i\downarrow} - \frac{1}{2} \right) + \mu \sum_{i,\sigma} \tilde{n}_{i\sigma} - 2\mu N_s, \end{aligned} \quad (5)$$

where

$$\tilde{t}_{ij} = \begin{cases} t & \text{if NN pairs are along } \pm \mathbf{a}_1 \text{ or } \pm \mathbf{a}_2, \\ -t & \text{if NN pairs are along } \pm \mathbf{a}_3, \end{cases} \quad (6)$$

reflecting the fact that the triangular lattice is tripartite. The different possibilities displayed in Eq. (6) indicate that there is no particle-hole symmetry, unless the hopping along  $\pm \mathbf{a}_3$  is disabled; this situation would be topologically equivalent to a square lattice. As a consequence,  $\mu = 0$  does not correspond to half-filling, as it does for bipartite lattices.

A *spin-down* particle-hole transformation<sup>13,14</sup> ( $\downarrow$ -PHT) leaves electrons with an up spin unchanged, while taking electrons with a down spin into holes:

$$c_{j\uparrow} \rightarrow \bar{c}_{j\uparrow} \quad \text{and} \quad c_{j\downarrow} \rightarrow \bar{c}_{j\downarrow}^\dagger = (-1)^j c_{j\downarrow}, \quad (7)$$

and their Hermitian conjugates, such that

$$n_{j\uparrow} \rightarrow \bar{n}_{j\uparrow} \quad \text{and} \quad n_{j\downarrow} \rightarrow \bar{n}_{j\downarrow} = 1 - n_{j\downarrow}. \quad (8)$$

The charge and spin degrees of freedom are exchanged under this transformation:

$$n_j \equiv n_{j\uparrow} + n_{j\downarrow} \rightarrow \bar{m}_j \equiv \bar{n}_{j\uparrow} - \bar{n}_{j\downarrow} = n_j - 1, \quad (9)$$

$$m_j \rightarrow \bar{n}_j = 1 + m_j. \quad (10)$$

The Hamiltonian (1) now becomes

$$\begin{aligned} \bar{\mathcal{H}} = & -t \sum_{\substack{(i,j) \\ \sigma}} \alpha_{ij}^\sigma \left( \bar{c}_{i\sigma}^\dagger \bar{c}_{j\sigma} + \text{H.c.} \right) \\ & - U \sum_i \left( \bar{n}_{i\uparrow} - \frac{1}{2} \right) \left( \bar{n}_{i\downarrow} - \frac{1}{2} \right) \\ & - \mu \sum_i \left( \bar{n}_{i\uparrow} - \bar{n}_{i\downarrow} \right) - \mu N_s, \end{aligned} \quad (11)$$

where

$$\alpha_{ij}^\sigma = \begin{cases} -1 & \text{if } \sigma = \downarrow \text{ and the NN pairs are along } \pm \mathbf{a}_3, \\ 1 & \text{otherwise.} \end{cases} \quad (12)$$

Similarly to bipartite lattices, the attractive model is equivalent to a repulsive model with chemical potential  $\bar{\mu} = 0$ , in the presence of a magnetic field  $h = 2\mu$ . Also, as discussed previously,<sup>7,8</sup> pairing and charge-density-wave (CDW) correlations associated with the attractive model become, respectively, planar (i.e.,  $xx$  and  $yy$ ) and  $zz$  staggered magnetization correlations in the repulsive model. The peculiar features introduced by the triangular lattice are (i) the hopping term is spin and direction dependent, and (ii) the repulsive model is not necessarily at half-filling, due to the absence of particle-hole symmetry at  $\bar{\mu} = 0$ .

The strong-coupling limit of the attractive model can be obtained<sup>14</sup> through perturbation theory in the space of doubly occupied states; these are compatible with any band filling and represent singlet pairing of electrons in real space. While to first order the hopping term gives zero contribution, to second order it induces transitions into virtual states with one broken pair. The effective Hamiltonian acting on this space is then

$$\begin{aligned} \mathcal{H}_{\text{eff}} = & - \frac{t^2}{|U|} \sum_{(i,j)} \left[ c_{i\sigma}^\dagger c_{j\sigma} c_{j\sigma}^\dagger c_{i\sigma} + c_{j-\sigma}^\dagger c_{i-\sigma} c_{i-\sigma}^\dagger c_{j\sigma} \right. \\ & \left. + (i \leftrightarrow j) \right] \\ & - \mu \sum_i (n_{i\uparrow} - n_{i\downarrow}), \end{aligned} \quad (13)$$

where  $(i \leftrightarrow j)$  replaces the preceding expression with labels  $i$  and  $j$  exchanged, since each pair of sites only appears once in the sum.

A spin representation for  $\mathcal{H}_{\text{eff}}$  is introduced through the definitions

$$S_i^z = \frac{1}{2}(n_{i\uparrow} + n_{i\downarrow} - 1), \quad (14a)$$

$$S_i^+ = c_{i\downarrow} c_{i\uparrow} = S_i^x + i S_i^y, \quad S_i^- \equiv (S_i^+)^{\dagger}, \quad (14b)$$

and

$$\sigma_i = \frac{1}{2}(n_{i\uparrow} - n_{i\downarrow}). \quad (14c)$$

One should not be misled by this notation, since  $S_i^z$  and  $\sigma_i$ , respectively, describe the charge and spin contents of site  $i$ . Since  $\sigma_i$  is identically zero in the space of doubly occupied states, the spin Hamiltonian becomes

$$\mathcal{H}_{\text{eff}} = J \sum_{(i,j)} \left( S_i^z S_j^z - \mathbf{S}_i^{\parallel} \cdot \mathbf{S}_j^{\parallel} \right) - h \sum_i S_i^z, \quad (15)$$

where  $J = 4t^2/|U|$ ,  $h = 2\mu$ ,  $\mathbf{S}_i^{\parallel} \equiv (S_i^x, S_i^y)$ , and a constant term has been dropped. The system then corresponds to a Heisenberg model in which the  $z$  components of  $\mathbf{S}$  couple antiferromagnetically and the planar components couple ferromagnetically. Therefore, CDW and singlet  $s$ -wave pairing correlations (SS) in the original model, respectively, correspond to staggered  $S^z$  and uniform  $\mathbf{S}^{\parallel}$  correlations in the spin representation. For zero field, the ground state of a pair of classical spins subject to this interaction corresponds to their respective  $x$  and  $y$

components of  $\mathbf{S}$  being parallel and to their  $z$  components being antiparallel, for any canting angle. Since the triangular lattice introduces frustration, the global minimum energy is achieved through a canting angle  $\theta = \pi/2$  (measured with respect to the  $z$  direction) or  $\langle S^z \rangle = 0$ . The lack of CDW ordering should also hold in the presence of quantum fluctuations, since their role is to decrease any tendency of ordering. Thus, unlike the square lattice,<sup>7,8</sup> one should not expect pairing and CDW correlations to coexist on the triangular lattice for any filling; we will return to this point in Sec. IV. It is worth mentioning that the ferromagnetic arrangement of  $\mathbf{S}^{\parallel}$  is favored up to a critical transverse field, a rough estimate of which is obtained through mean-field arguments as  $h_c \sim zJ$ , where  $z$  is the coordination number of the lattice.

Since an SS state is associated with planar ordering, the transition is of the Kosterlitz-Thouless type,<sup>15</sup> and the low-lying excitations are gapless, corresponding to pseudo-spin-waves.<sup>14</sup> That is, they do not correspond to configurations with broken pairs, which would imply a gap of order  $\sim |U|$ . The latter is commonly referred to as a *spin gap* and is probed at an energy scale larger than  $T_c$ .<sup>1,11</sup> As the temperature is decreased, the superconducting transition is then thought of as a condensation of preformed local pairs.<sup>1</sup>

It is also instructive to discuss the strong-coupling limit of the equivalent repulsive model, Eq. (11). Second-order perturbation theory on the basis of singly occupied states—thus valid at half-filling—leads to an effective spin Hamiltonian<sup>14</sup>

$$\tilde{\mathcal{H}}_{\text{eff}} = J \sum_{\langle i,j \rangle} S_i^z S_j^z + \sum_{\langle ij \rangle} J_{ij}^{\parallel} \mathbf{S}_i^{\parallel} \cdot \mathbf{S}_j^{\parallel} - h \sum_i S_i^z, \quad (16)$$

where  $J = 4t^2/|U|$  as before, and

$$J_{ij}^{\parallel} = \begin{cases} -J & \text{if the NN pairs are along } \pm \mathbf{a}_3, \\ J & \text{otherwise.} \end{cases} \quad (17)$$

The spin operators are related to the fermion operators appearing in (11) through

$$S_i^z = \frac{1}{2}(\bar{n}_{i\uparrow} - \bar{n}_{i\downarrow}), \quad (18a)$$

$$S_i^+ = \bar{c}_{i\uparrow}^\dagger c_{i\downarrow} = S_i^x + iS_i^y, \quad S_i^- \equiv (S_i^+)^\dagger, \quad (18b)$$

and

$$\sigma_i = \frac{1}{2}(\bar{n}_{i\uparrow} + \bar{n}_{i\downarrow} - 1). \quad (18c)$$

Alternatively, the same result is obtained if one performs a  $\downarrow$ -PHT directly on the strong-coupling limit of the attractive model. Taking Eqs. (7) into (14), the spin operators are transformed as

$$S_i^\pm \rightarrow (-1)^i S_i^\pm, \quad S_i^z \rightarrow S_i^z, \quad (19)$$

so that Eq. (15) is taken into Eq. (16). Again, the model given by Eq. (16) is such that only the  $z$  component of  $\mathbf{S}$ , which in this case also describes the charge degrees of freedom, is frustrated. The conclusions of this section are based on a strong-coupling analysis. In Sec. IV these

results will be checked against those of quantum Monte-Carlo simulations for intermediate couplings.

### III. QUANTUM MONTE CARLO AND FINITE-SIZE SCALING

In a grand-canonical simulation<sup>16–19</sup> the imaginary time is discretized through the introduction of  $M$  “time” slices separated by an interval  $\Delta\tau$  such that  $\beta \equiv \Delta\tau M$ . The partition function is then written as

$$Z = \text{Tr} e^{-\Delta\tau M \mathcal{H}} \simeq \text{Tr} (e^{-\Delta\tau \mathcal{K}} e^{-\Delta\tau \mathcal{V}})^M, \quad (20)$$

with

$$\mathcal{K} = -t \sum_{\langle i,j \rangle} (c_{i\sigma}^\dagger c_{j\sigma} + \text{H.c.}) - \mu \sum_{i,\sigma} n_{i\sigma} \quad (21)$$

and

$$\mathcal{V} = U \sum_i (n_{i\uparrow} - \frac{1}{2})(n_{i\downarrow} - \frac{1}{2}). \quad (22)$$

The last step in Eq. (20) follows from the Trotter formula.<sup>20</sup> The systematic errors are of order  $\Delta\tau^2$  in the measured quantities; one therefore wishes to take  $\Delta\tau$  as small as possible, though compatible with a moderate number of time slices, say  $M \lesssim 80$ .

A discrete Hubbard-Stratonovich (HS) transformation<sup>21</sup> is performed for each on-site interaction term,

$$e^{-\Delta\tau U (n_{i\uparrow} - 1/2)(n_{i\downarrow} - 1/2)} = \frac{1}{2} e^{-\Delta\tau U/4} \text{Tr}_{s_{i\ell}} e^{-\Delta\tau \lambda s_{i\ell} (n_{i\uparrow} + n_{i\downarrow} - 1)}, \quad (23)$$

where a new Ising field  $s_{i\ell} = \pm 1$  has been introduced, and  $\cosh \lambda \Delta\tau = e^{-\Delta\tau U/2}$ . Defining  $N_s \times N_s$  matrices  $\mathbf{K}$  and  $\mathbf{V}(\ell)$  such that

$$K_{ij} = \begin{cases} -t & \text{if } i, j \text{ are NN sites,} \\ 0 & \text{otherwise,} \end{cases} \quad (24)$$

and

$$V_{ij}(\ell) = \delta_{ij} \left\{ \frac{1}{2} \lambda s_{i\ell} - \mu \right\}, \quad (25)$$

we can write

$$Z = \left( \frac{1}{2} e^{-\Delta\tau U/4} \right)^{N_s M} \text{Tr}_{\{s\}} \text{Tr} \prod_{\sigma} \prod_{\ell} D_{\ell}^{\sigma}, \quad (26)$$

where  $N_s$  is the number of lattice sites, and

$$D_{\ell}^{\sigma} = e^{-\Delta\tau \sum_{ij} K_{ij} c_{i\sigma}^\dagger c_{j\sigma}} e^{-\Delta\tau \sum_{ij} V_{ij}(\ell) c_{i\sigma}^\dagger c_{j\sigma}}. \quad (27)$$

The fermion degrees of freedom can be traced over<sup>16,17,19</sup> to yield

$$Z = \text{Tr}_{\{s\}} (\det \mathbf{O})^2, \quad (28)$$

since both  $\mathbf{K}$  and  $\mathbf{V}$  are independent of  $\sigma$ , and in a “space” formulation,<sup>16,17</sup>

$$O = \mathbb{1} + B_M B_{M-1} \cdots B_1, \quad (29)$$

with

$$B_\ell = e^{-\Delta\tau K} e^{-\Delta\tau V(\ell)}. \quad (30)$$

At this point one should stress that the ‘‘Boltzmann weight’’  $P(\{s\}) = (\det O)^2$  is positive, which makes the simulation on the attractive Hubbard model free from ‘‘minus sign’’ problems.<sup>18,19</sup> In order to stabilize the simulations at low temperatures, instead of (29) we use a ‘‘space-time’’ formulation,<sup>22</sup> in which  $M_0$  consecutive time slices are collapsed to construct a matrix  $O_{M_0}$ , of order  $pN_s \times pN_s$ , with  $p = M/M_0$ ; see Ref. 22 for details. With this algorithm advance, we are able to reach inverse temperatures as large as  $\beta = 10/t$ .

The heat-bath algorithm is used to sample the auxiliary Ising fields subject to the ‘‘Boltzmann weight’’  $P(\{s\})$ , the ratio of which is related to the equal time Green’s function  $g_{ij}^\sigma(\ell) \equiv \langle c_{i\sigma}(\ell\Delta\tau) c_{j\sigma}^\dagger(\ell\Delta\tau) \rangle$ ; the imaginary-time dependence of the operators is given by  $a(\tau) \equiv e^{\tau\mathcal{H}} a e^{-\tau\mathcal{H}}$ . If the new configuration is accepted, the Green’s function is updated through simple operations;<sup>16–19,22</sup> the thermodynamic expectation values are also expressed in terms of Green’s functions.<sup>16–19,22</sup> Here we examine quantities such as the equal-time  $\mathbf{q} = \mathbf{0}$  local (or  $s$ -wave) pairing correlation function

$$P_s(T, L) \equiv \langle \Delta^\dagger \Delta + \Delta \Delta^\dagger \rangle, \quad (31)$$

where  $T$  is the temperature,  $L$  is the linear lattice size, and

$$\Delta^\dagger = \frac{1}{L} \sum_i c_{i\uparrow}^\dagger c_{i\downarrow}^\dagger, \quad (32)$$

and the equal-time charge-density structure factor

$$C(\mathbf{q}) \equiv \langle n_{\mathbf{q}} n_{\mathbf{q}}^\dagger \rangle, \quad (33)$$

with

$$n_{\mathbf{q}}^\dagger = \frac{1}{L} \sum_i e^{i\mathbf{q}\cdot\mathbf{r}_i} (n_{i\uparrow} + n_{i\downarrow}). \quad (34)$$

We also calculate the uniform magnetic susceptibility

$$\chi(\mathbf{0}) = \frac{1}{N_s} \sum_{ij} \int_0^\beta d\tau \langle m_i(\tau) m_j(0) \rangle, \quad (35)$$

with

$$m_i(\tau) = e^{\tau\mathcal{H}} [n_{i\uparrow} - n_{i\downarrow}] e^{-\tau\mathcal{H}}. \quad (36)$$

The dependence of the pairing correlation function with the system size can be extracted through finite-size scaling (FSS) arguments.<sup>23</sup> For an infinite two-dimensional system, one expects a superconducting transition within the Kosterlitz-Thouless<sup>15</sup> XY-model universality class. Therefore, pairing correlations become critical at the critical temperature  $T_c$ , and decay algebraically,

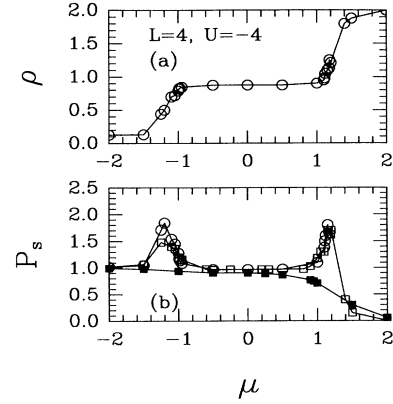


FIG. 1. Occupation (a) and pairing correlations (b) as functions of the chemical potential with  $U = -4$ , for a lattice with  $L = 4$ . Solid squares represent data for  $\beta = 2$ , open squares for  $\beta = 5$ , and circles for  $\beta = 7$ . The error bars are smaller than the data points, and the solid lines are guides to the eye.

$$G(r) \sim r^{-\eta}, \quad (37)$$

where  $\eta = 0.25$  for  $T \rightarrow T_c^+$ . For a finite system of size  $L$ , its associated uniform Fourier transform becomes

$$P_s \sim \int_0^L d^2r r^{-\eta} \sim L^{2-\eta}. \quad (38)$$

Above criticality, the appropriate scaling variable<sup>23</sup> is  $L/\xi$ , where  $\xi \sim \exp(A/\sqrt{T - T_c})$ , with  $A$  being of order unity, is the correlation length for the infinite system. Therefore, one can assume the following FSS ansatz:

$$P_s(T, L) = L^{2-\eta} F(L/\xi), \quad (39)$$

where  $F(z)$  is a scaling function such that  $F(z) \rightarrow \text{const}$  when  $L \ll \xi$ , recovering Eq. (38). At  $T_c$ ,  $\xi = \infty$ , so that  $L^{\eta-2} P_s(T_c, L)$  is a constant independent of lattice size. By plotting  $L^{\eta-2} P_s(T, L)$  as a function of  $T$  for systems of different sizes, an estimate of  $T_c$  can be obtained as the temperature where two successive curves intercept.<sup>24</sup> Similar arguments can be used with any other thermodynamic quantity.

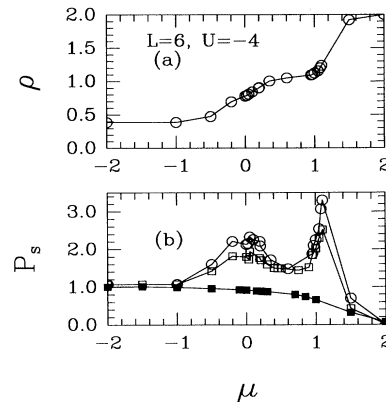


FIG. 2. Same as Fig. 1, but for a lattice with  $L = 6$ .

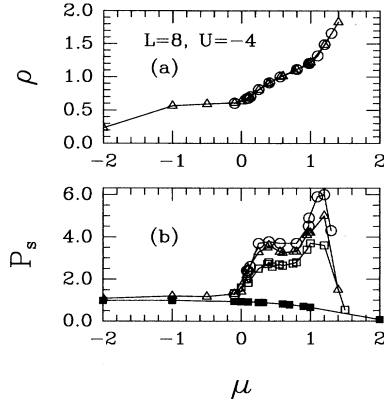


FIG. 3. Occupation (a) and pairing correlations (b) as functions of the chemical potential with  $U = -4$ , for a lattice with  $L = 8$ . Solid squares represent data for  $\beta = 2$ , open squares for  $\beta = 5$ , open triangles for  $\beta = 6$ , and circles for  $\beta = 7$ . The error bars are smaller than the data points, and the solid lines are guides to the eye.

#### IV. RESULTS AND DISCUSSION

The triangular lattice clusters used here have  $N_s = L \times L$  sites, with periodic boundary conditions; that is, each site is connected with its six nearest neighbors through a hopping term. The simulations were performed on Sun work stations; a single datum point involves between 500 and 1000 MC sweeps over all time slices, and we took  $\Delta\tau = 0.125$ . From now on, energies will be expressed in units where the hopping  $t = 1$ , and we also set the Boltzmann constant  $k_B = 1$ . In a grand-canonical

simulation, one adjusts the chemical potential to obtain the desired occupation,  $\rho \equiv \langle n \rangle$ . Figures 1–3 show the behavior of  $\rho$  and  $P_s$  versus  $\mu$  for  $U = -4$ ; for the sake of clarity, the data for  $\rho$  are shown for a single value of  $\beta$  in Figs. 1 and 2 and for two values in Fig. 3. One should note from the outset that the results with lattice size  $L = 4$  behave quite distinctly from those with  $L = 6$  and 8. For instance, the compressibility,

$$K = \frac{1}{\langle n \rangle^2} \frac{\partial \langle n \rangle}{\partial \mu}, \quad (40)$$

vanishes at low temperatures for a wide range of  $\mu$  near  $\mu = 0$  only for  $L = 4$ ; see Figs. 1(a), 2(a), and 3(a). Also, the two peaks in  $P_s$  have similar heights and are farther apart when  $L = 4$ . We can therefore consider the triangular lattice with  $L = 4$  too small to be helpful in estimating  $T_c$  within a FSS analysis, and will not use the data with  $L = 4$  throughout the rest of this work.

Figure 4 shows the size-scaled pairing correlation, Eq. (31), as a function of the inverse temperature, for  $U = -4$  and for several band fillings; the error bars are of the order of the data points. For  $\rho = 0.7$  [Fig. 4(a)] the curves do not intercept, at least up to  $\beta \sim 10$ ; thus  $T_c$  could be between 0 and 0.1, in this case. On the other hand, one can define a  $\beta_c(\rho)$  for  $\rho \in [0.8, 1.2]$ , as the value where the data points superimpose. Taking into account the error bars for the data points, we see that this criterion generally implies an error  $\Delta\beta_c \sim \pm 1$ , except for  $\langle n \rangle = 1.2$ , for which this error can be as large as 3. These estimates are plotted in the phase diagram of Fig. 5. It should be stressed that the error bars in Fig. 5 are merely indicative of the location of  $T_c$  for a given pair of different sized systems; they do not refer to any

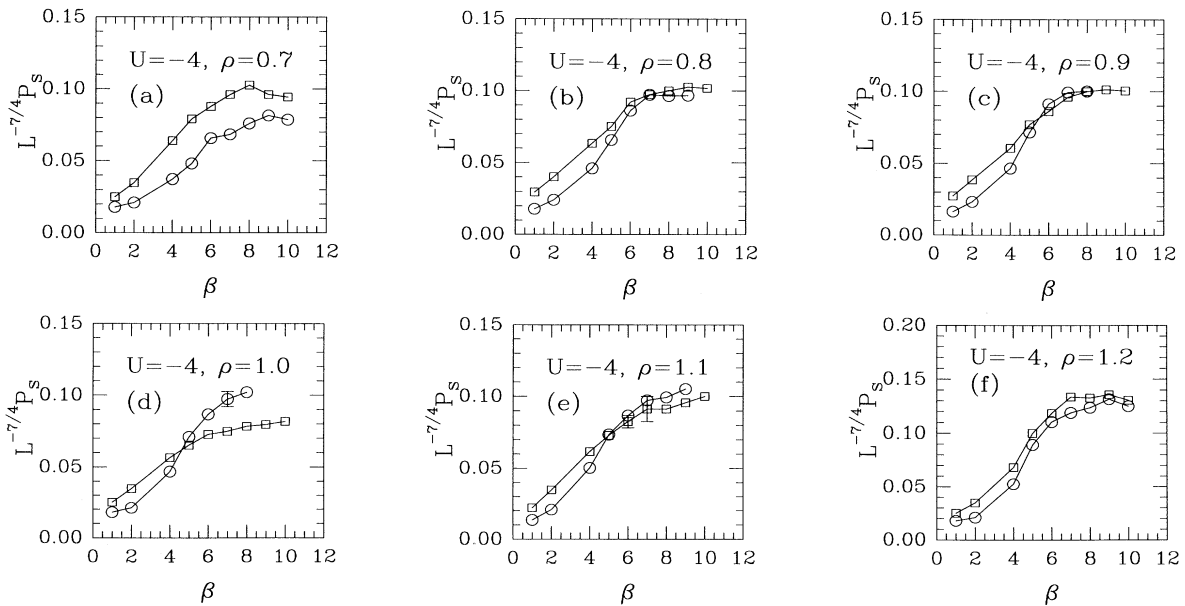


FIG. 4. Size-scaled  $\mathbf{q} = \mathbf{0}$  Fourier transform of the  $s$ -wave pairing correlation function as a function of the inverse temperature, for lattices with  $L = 6$  (squares) and  $L = 8$  (circles), and for different band fillings: (a)  $\rho = 0.7$ , (b)  $\rho = 0.8$ , (c)  $\rho = 0.9$ , (d)  $\rho = 1.0$ , (e)  $\rho = 1.1$ , and (f)  $\rho = 1.2$ ;  $U = -4$  in all cases. Except where shown, the error bars are smaller than the data points; the solid lines are guides to the eye.

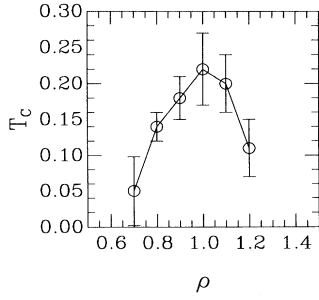


FIG. 5. Critical temperature as a function of the band filling, for  $U = -4$ . The error bars reflect the uncertainty in the location of the crossings in Fig. 4, and the solid line is a guide to the eye.

extrapolation to the thermodynamic limit.

Before comparing with the square lattice, let us examine CDW correlations. In Fig. 6 we show  $C(\mathbf{q})$  as defined by Eq. (33), for fixed band filling, temperature, and  $U$ . The lack of scaling with size is evident, since the results for  $L = 8$  are practically the same as for  $L = 6$ ; the situation for other fillings is very much the same. These results confirm the strong-coupling prediction of Sec. II, according to which charge-density-wave correlations were frustrated and should be suppressed for any filling on a triangular lattice.

The phase diagram of Fig. 5 is similar to the one for the square lattice<sup>8</sup> in the sense that it displays a maximum. The lack of CDW ordering, however, makes the order parameter two dimensional for any filling; in particular, the maximum  $T_c$  for the triangular lattice is near half-filling. This is in marked contrast to the square lattice, for which the order parameter is three dimensional at half-filling, pressing  $T_c$  for superconductivity down to zero for  $\rho = 1$ . Also, the maximum critical temperature for the triangular lattice is  $T_c^*(\text{triang}) \simeq 0.2$ , which is higher than its square lattice counterpart,  $T_c^*(\text{square}) \simeq 0.1$ ; this should be expected due to the larger coordination number of the former lattice. At this point we cannot give any numerical estimates for  $T_c$  outside the occupation interval  $[0.7, 1.2]$  as it would require simulations at much lower temperatures.

In order to check the behavior with  $U$ , we have also de-

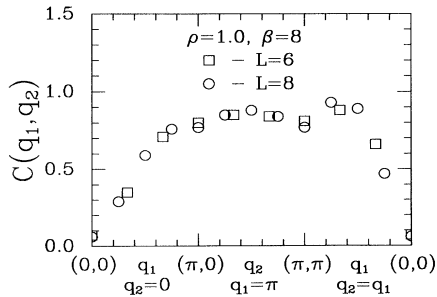


FIG. 6. Charge-density structure factor at half-filling,  $U = -4$ , and inverse temperature  $\beta = 8$ . Squares and circles represent data for lattices with  $L = 6$  and  $L = 8$ , respectively.

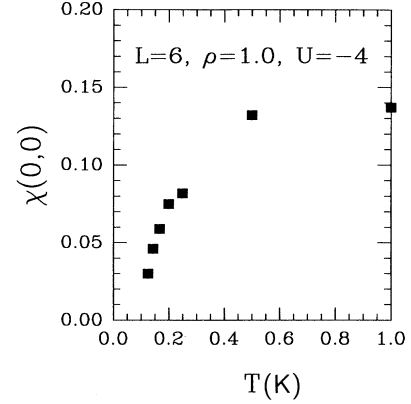


FIG. 7. Uniform susceptibility as a function of temperature for  $U = -4$  at half-filling for a lattice with  $L = 6$ .

termined the critical temperature for  $\rho = 0.9$  and  $U = -6$  to be  $T_c \simeq 0.25$ . One should expect the whole phase diagram to be pushed upwards in temperature, in analogy with the square lattice, though a somewhat greater computational effort would be required to investigate the location of the maximum with  $U$ .

Finally, we now discuss the uniform magnetic susceptibility and the spin gap. We recall that in the weak-coupling regime the transition is from a normal (Fermi liquid) metal to a (BCS) superconductor,<sup>1</sup> the transition temperature being exponentially small,  $T_c \sim W \exp(-W/|U|)$ , where  $W = 6zt$  is one half of the bandwidth. One would therefore expect the uniform susceptibility  $\chi(0,0)$  to display a weak temperature dependence at low temperatures. For stronger couplings, on the other hand, local pairs are formed at temperatures quite higher than  $T_c$ , though without coherence.<sup>1</sup> In this regime the spin excitations correspond to a breaking of these pairs, with an energy cost (gap) of order  $|U|$ . The formation of local pairs, and the associated spin gap, should be reflected in the magnetic properties: A local bound pair must have a smaller response to a uniform field than isolated fermions. The uniform susceptibility should then be strongly suppressed as the temperature is lowered in the region of strong coupling. This picture is consistent with the discussion in Ref. 11, in which a region of concave susceptibility is associated with a spin gap. We present in Fig. 7 the uniform susceptibility as a function of temperature for the  $L = 6$  lattice at half-filling and  $U = -4$ . The suppression is apparent for  $T \lesssim 0.5$ , quite higher than the estimated critical temperature,  $T_c \simeq 0.2$  in this case; at  $T_c$  the preformed pairs condense, not necessarily affecting the behavior of  $\chi(0,0)$  any further. We are led to conclude from Fig. 7 that the spin gap is not suppressed by frustration. A similar behavior is found for other fillings.

## V. CONCLUSIONS

We have examined the influence of lattice topology on the properties of the attractive (i.e., negative- $U$ ) Hub-

bard model. In particular, we have studied local pairing, charge-density-wave correlations, and the uniform magnetic susceptibility on a triangular lattice. The strong-coupling limit is equivalent to a Heisenberg model with ferromagnetic couplings between the planar ( $x$  and  $y$ ) components of the spin operators, and to a frustrated antiferromagnetic coupling between the  $z$  components. Since correlations between  $z$  components describe charge correlations, CDW order cannot set in due to frustration. Quantum Monte Carlo results confirm the absence of CDW correlations at intermediate couplings, and show that superconducting ordering is favored at half-filling. Further, our results for the uniform magnetic susceptibil-

ity suggest that the precursor (normal) spin-gap phase is not affected by frustration.

#### ACKNOWLEDGMENTS

The author is grateful to M. A. Continentino for useful discussions. Financial support from the Brazilian Agencies, Ministério de Ciência e Tecnologia, Conselho Nacional de Desenvolvimento Científico e Tecnológico (CNPq), and Coordenação de Aperfeiçoamento do Pessoal de Ensino Superior (CAPES) is also gratefully acknowledged.

\* Electronic address: rrrds@fis.puc-rio.br

- <sup>1</sup> R. Micnas, J. Ranninger, and S. Robaszkiewicz, *Rev. Mod. Phys.* **62**, 113 (1990).
- <sup>2</sup> P. W. Anderson, *Phys. Rev. Lett.* **34**, 953 (1976).
- <sup>3</sup> V. L. Ginzburg, *Zh. Eksp. Teor. Fiz.* **47**, 2318 (1964) [*Sov. Phys. JETP* **20**, 1549 (1965)].
- <sup>4</sup> W. A. Little, *Phys. Rev. A* **134**, 1416 (1964).
- <sup>5</sup> J. E. Hirsch and D. J. Scalapino, *Phys. Rev. B* **32**, 5639 (1985).
- <sup>6</sup> C. S. Ting, K. L. Nagai, and C. T. White, *Phys. Rev. B* **22**, 2318 (1980).
- <sup>7</sup> R. T. Scalettar, E. Y. Loh, J. E. Gubernatis, A. Moreo, S. R. White, D. J. Scalapino, R. L. Sugar, and E. Dagotto, *Phys. Rev. Lett.* **62**, 1407 (1989).
- <sup>8</sup> A. Moreo and D. J. Scalapino, *Phys. Rev. Lett.* **66**, 946 (1991).
- <sup>9</sup> H. E. Castillo and C. A. Balseiro, *Phys. Rev. B* **45**, 10549 (1992).
- <sup>10</sup> R. R. dos Santos, *Phys. Rev. B* **46**, 5496 (1992).
- <sup>11</sup> M. Randeria, N. Trivedi, A. Moreo, and R. T. Scalettar, *Phys. Rev. Lett.* **69**, 2001 (1992).
- <sup>12</sup> F. C. Zhang, M. Ogata, and T. M. Rice, *Phys. Rev. Lett.* **67**, 3452 (1991).
- <sup>13</sup> H. Shiba, *Prog. Theor. Phys.* **48**, 2171 (1972).
- <sup>14</sup> V. J. Emery, *Phys. Rev. B* **14**, 2989 (1976).
- <sup>15</sup> J. M. Kosterlitz and D. J. Thouless, *J. Phys. C* **6**, 1181 (1973).
- <sup>16</sup> R. Blankenbecler, D. J. Scalapino, and R. L. Sugar, *Phys. Rev. D* **24**, 2278 (1981).
- <sup>17</sup> J. E. Hirsch, *Phys. Rev. B* **31**, 4403 (1985).
- <sup>18</sup> E. Y. Loh, Jr. and J. E. Gubernatis, in *Electronic Phase Transitions*, edited by W. Hanke and Yu. V. Kopayev (Elsevier, Amsterdam, 1992).
- <sup>19</sup> W. von der Linden, *Phys. Rep.* **220**, 53 (1992).
- <sup>20</sup> M. Suzuki, *Prog. Theor. Phys.* **56**, 1454 (1976).
- <sup>21</sup> J. E. Hirsch, *Phys. Rev. B* **28**, 4059 (1983).
- <sup>22</sup> J. E. Hirsch, *Phys. Rev. B* **38**, 12023 (1988).
- <sup>23</sup> M. E. Fisher, in *Critical Phenomena*, Proceedings of the International School of Physics "Enrico Fermi," Course LI, Varenna, 1970, edited by M. S. Green (Academic, New York, 1971); M. N. Barber, in *Phase Transitions and Critical Phenomena*, edited by C. Domb and J. L. Lebowitz (Academic, London, 1983), Vol. 8.
- <sup>24</sup> M. P. Nightingale, *J. Appl. Phys.* **53**, 7927 (1982); R. R. dos Santos and L. Sneddon, *Phys. Rev. B* **23**, 3541 (1981).